Nonlinear optical response of Ge nanocrystals in a silica matrix

A. Dowd[a] and R. G. Elliman
Department of Electronic Materials Engineering, Research School of Physical Sciences and Engineering, Institute of Advanced Studies, Australian National University, Canberra ACT 0200, Australia

M. Samoc and B. Luther-Davies
Australian Photonics Cooperative Research Centre, Laser Physics Centre, Research School of Physical Sciences and Engineering, Institute of Advanced Studies, Australian National University, Canberra ACT 0200, Australia

(Received 24 June 1998; accepted for publication 6 November 1998)

Time-resolved degenerate-four-wave-mixing measurements were used to study the nonlinear optical response (intensity-dependent refractive index) of Ge nanocrystallites embedded in a silica matrix. Nanocrystals were fabricated by ion-implanting silica with 1.0 MeV Ge ions to fluences in the range from 0.6 to 3×10^{17} Ge cm^{-2}, followed by annealing at 1100 °C for 60 min. For the highest fluence, this resulted in nanocrystals with a log-normal size distribution, having a geometric mean diameter of 3.0 nm and a dimensionless geometric standard deviation of 0.25. The intensity-dependent refractive index $|n_2|$ was measured at a wavelength of 800 nm and found to increase linearly with increasing Ge fluence. For the highest fluence, $|n_2|$ was determined to be in the range 2.7–6.9 $\times10^{-13}$ cm^{-2} W^{-1}, depending on the duration of the excitation pulse; values were consistently smaller for shorter pulse lengths. Relaxation of the nonlinear response was found to have two characteristic time constants, one <100 fs and the other ~1 ps. © *1999 American Institute of Physics.* [S0003-6951(99)04802-0]

The development of materials with novel linear and nonlinear optical properties is the key to realizing the full potential of all-optical computing and signal processing. In this context, it is well known that glasses containing metal particles, such as Au, Ag, and Cu, exhibit such novel properties due to local field enhancement near the surface plasmon resonance of the metal.[1] This results in resonant absorption, giving such materials a characteristic color, and in an increase in the third-order susceptibility, leading to an enhanced Kerr nonlinearity of such materials.[2–5] For Au, the optical nonlinearity arises from interband electric dipole transitions, hot-electron excitation, and thermal effects, where the relative contribution from the different processes depends on the excitation pulse length. For femtosecond excitation, interband transitions are important, with hot-carrier and thermal effects becoming increasingly important for increasing pulse lengths (ps–ns).[6] Glasses containing semiconductor nanocrystals also exhibit interesting optical properties, including tunable absorption, strong photo- and electroluminescence, and large third-order optical nonlinearities.[7–12] In this case, however, the understanding of the material response is less well developed.

Several techniques exist for producing semiconductor nanocrystals in dielectric matrices, including: sputtering,[13,14] chemical vapor deposition,[15,16] and ion implantation.[17,18] The latter technique provides considerable flexibility and is readily used in combination with planar waveguide technology to produce optical devices. In the present study, degenerate four-wave mixing was used to study the nonlinear optical response of Ge nanocrystals formed in fused silica by ion implantation and thermal annealing.

Fused silica (Infrasil) substrates, 40 mm long, 10 mm wide, and 1 mm thick, were implanted at −290 °C with 1.0 MeV Ge to fluences of 0.6, 1.0, 2.0, and 3.0 $\times10^{17}$ Ge cm^{-2}. The mean-projected range of the ions was 0.63 μm and the peak concentration was less than 10 at. % in all cases. Samples were subsequently annealed at 1100 °C for 60 min in a quartz tube furnace with a flowing forming-gas (5% H_2, 95% N_2) ambient. Physical characterization of the samples was undertaken with Rutherford backscattering spectrometry (RBS) using 2.0 MeV He ions (scattering angle of 168°) and by transmission electron microscopy (TEM) using a Philips 430 operating at 300 kV. Cross-sectional samples were prepared by mechanical polishing, dimpling, and ion milling.

Time-resolved degenerate-four-wave-mixing (DFWM) measurements were performed at a wavelength of 800 nm using amplified pulses from a Coherent MIRA 800-D femtosecond Ti:sapphire laser. The output beam was divided into three equal intensity beams (a probe beam and two pump beams), which were brought to a common temporal and spatial focus on the sample. The spatial extent of the beams at the sample surface was analyzed using a charge-coupled-device array and found to correspond to a full width at half maximum (FWHM) spot diameter of 130 μm (w_0 $=150\,\mu$m). The overlap length of the beams within the sample was estimated to be ~700 μm and the laser pulse duration was varied in the range from 100 fs to 1 ps (FWHM), as determined by autocorrelation measurements. The relaxation time of the nonlinear response was determined by delaying the probe beam relative to the pump beams. The laser pulse energy employed for the present measurements was up to 6 μJ per pulse, and importantly, the pulse repetition rate was only 30 Hz, reducing effects due to beam heating of the nanocrystals. Both phase-matched and non-phase-matched mixing signals were monitored, providing information on the response of the silica substrate and the implanted layer (see Ref. 19 for a discussion of the use of

[a]Electronic mail: ard109@rsphysse.anu.edu.au

 © 1999 American Institute of Physics

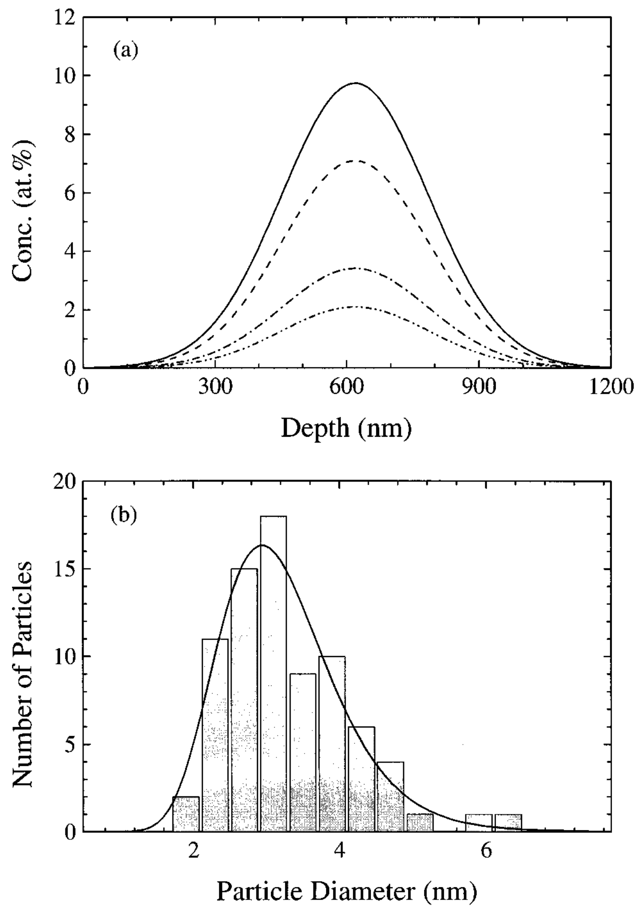

FIG. 1. (a) Ge distribution following implantation at 77 K. Curves correspond to fluences of: 0.6, 1.0, 2.0, and 3×10^{17} Ge cm^{-2}. (b) Distribution of particle sizes from TEM for Ge nanocrystals in SiO_2 implanted to a dose of 3×10^{17} Ge cm^{-2}.

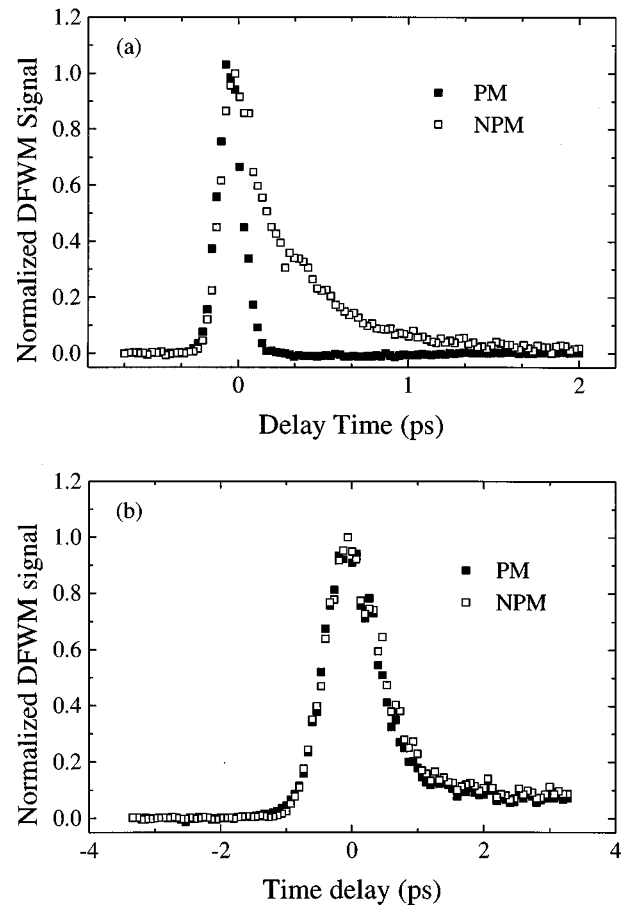

FIG. 2. DFWM data for a sample implanted with 3×10^{17} Ge cm^{-2} measured with a pulse width of (a) 100 fs and (b) 650 fs. Points represent phase-matched (open squares) and non-phase-matched (solid squares) signals normalized to unity.

non-phase-matched DFWM signals). Since the phase-matched signal was practically dominated by the nonlinear response of the silica substrate, $|n_2|$ (the intensity-dependent refractive index) of the implanted layer was determined from the ratio of the two signals, correcting for different effective sampling volumes, and taking $|n_2|$ for silica to be 3×10^{-16} cm^2/W, as used in Ref. 20.

Figure 1(a) shows the depth distribution of the implanted Ge obtained from RBS measurements; the projected range of the Ge ions is 630 nm and the full width at half maximum is 380 nm. The peak Ge concentrations vary from 1.5×10^{21} Ge cm^{-3} (2.1 at. %) to 6.8×10^{21} Ge cm^{-3} (9.7 at. %). These samples were subsequently annealed to 1100 °C to promote the growth of Ge crystallites. The resulting size distribution of the nanocrystals is shown in Fig. 1(b) for the sample implanted with 3×10^{17} Ge cm^{-2}. This distribution, determined from TEM images, is well represented by a log-normal function with a geometric mean diameter of 3.0 nm and a dimensionless geometric standard deviation of 0.25. The depth distribution of Ge was unaffected by the anneal and this size distribution represents an average of the particle diameters over all depths. Note that particles of the order of 3.0 nm are predicted to have a band gap significantly larger than that of bulk Ge due to quantum confinement effects.[21]

Figure 2 shows phase-matched and non-phase-matched DFWM signals for the sample implanted with 3×10^{17} Ge cm^{-2} [i.e., the same sample for which the size distribution was determined in Fig. 1(b)]. Measurements were performed with two different pulse durations, 100 fs shown in Fig. 2(a), and 650 fs shown in Fig. 2(b). The pulse energy was 6 μJ in both cases. (Note that the phase-matched and non-phased-matched signals have been normalized to the same height to aid presentation.) $|n_2^{\mathrm{Ge}}|$ is calculated from the actual peak heights using the equation:

$$|n_2^{\mathrm{Ge}}|^2=k\left(\frac{I^{\mathrm{Ge}}}{I^{\mathrm{silica}}}\right)\left(\frac{I_{\mathrm{ref}}^{\mathrm{silica}}}{I_{\mathrm{ref}}^{\mathrm{Ge}}}\right)^3\left(\frac{L^{\mathrm{silica}}}{L^{\mathrm{Ge}}}\right)^2|n_2^{\mathrm{silica}}|^2, \quad (1)$$

where n_2^{Ge} is the nonlinear index of the Ge-implanted layer; I^{Ge} is the measured non-phase-matched DFWM signal; I^{silica} is the phase-matched DFWM signal from a reference sample (unimplanted silica); L^{Ge} is the effective sampling length for the Ge-implanted layer; taken to be the FWHM of the Ge distribution, 380 nm; and L^{silica} is the effective sampling length in the silica substrate, determined to be 700 μm. $I_{\mathrm{ref}}^{\mathrm{Ge}}$ and $I_{\mathrm{ref}}^{\mathrm{silica}}$ are measured signals proportional to the intensity incident on the Ge- and unimplanted samples, respectively. k is an experimental calibration factor that allows for variations in detector responses and beam intensities, and accounts for the fact that the phase-matched and non-phase-matched signals derive from different contributions. For the measurements shown in Fig. 2, $|n_2^{\mathrm{Ge}}|$ was determined to be 2.7×10^{-13} and 6.9×10^{-13} cm^2 W^{-1}, for the 100 and 650 fs pulses, respectively, i.e., $|n_2^{\mathrm{Ge}}|$ increases with increasing pulse duration.

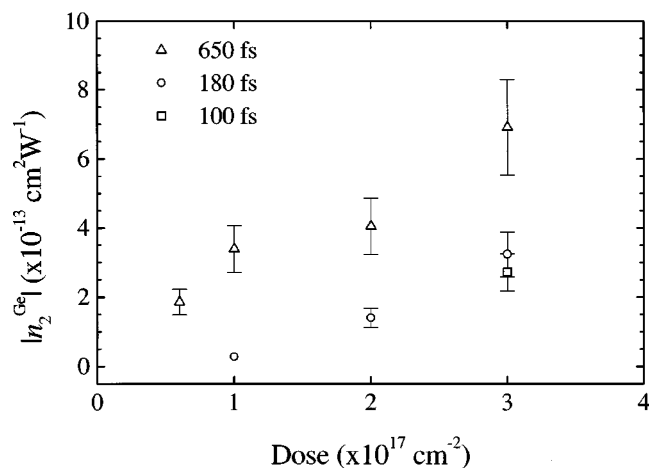

FIG. 3. Nonlinear refractive index $|n_2^{Ge}|$ plotted as a function of implanted dose for different excitation pulse lengths.

The variation with pulse length is also evident in Fig. 3, which shows $|n_2^{Ge}|$ as a function of ion fluence measured with pulses of 100, 180, and 650 fs duration: $|n_2^{Ge}|$ is consistently smaller for the shorter pulse durations. These data also show that $|n_2^{Ge}|$ increases linearly with increasing ion fluence over the range from 0.6 to $3\times10^{17}\,\mathrm{Ge\,cm^{-2}}$, and that this dependence is similar for measurements made with pulse durations of 180 and 650 fs. [Optical absorption in these films also increases linearly with ion fluence (data not shown), suggesting that the nonlinearity is absorptive rather than refractive, a conclusion which is supported by preliminary *Z*-scan (Ref. 12) measurements.] It is found that $|n_2^{Ge}|$ determined from Eq. (1) is independent of pulse power over a range spanning the current measurements. This implies that the nonlinearity scales with the third power of the intensity, i.e., a Kerr nonlinearity.

In bulk Ge, absorption at 800 nm (1.56 eV) is primarily due to $\Gamma'_{25}-\Gamma'_2$ ($\Delta E\sim0.8$ eV) transitions, with $\Gamma'_{25}-\Gamma'_{15}$ transitions ($\Delta E\sim2.7-3.6$ eV) potentially contributing through two-photon absorption.[22] Quantum confinement effects are expected to increase the band gap of Ge nanocrystals, suggesting that absorption should be dominated by single-photon absorption in the present case, i.e., the $\Gamma'_{25}-\Gamma'_2$ transition. This assumes that the crystallites have a well-defined bulk-like band structure and that defect states do not contribute to the absorption process. However, defects may contribute to the nonlinear response of semiconductor nanocrystals by providing alternative channels for carrier excitation and relaxation. This is consistent with the fact that relatively large nonlinearities are measured for Si nanocrystals in silica, even though the photon energy is less than the direct gap of bulk Si:[12] $|n_2|$ for Si is 30% of that for Ge nanocrystals, whereas the absorption coefficients for the bulk phases differ by more than a factor of 50.

Temporal relaxation of the nonlinearity is shown in Fig. 2(a), highlighting at least two distinct relaxation times: an instantaneous response (with a relaxation time <100 fs) and a slower response with a relaxation time of 0.8–1.0 ps. [Earlier measurements on unannealed samples using 100 fs pulses showed relaxation times of <100 fs and 1.1 ps (Ref. 12).] Carrier lifetimes are typically of the order of 10^{-3} s in pure Si and Ge, which is much longer than those observed in the present case. However, the presence of impurities and defects can significantly reduce carrier lifetimes. For example, ion-irradiated Si can exhibit carrier lifetimes $\leqslant1$ ps,[23] and Ge is expected to behave similarly. It is, therefore, plausible that the measured ~1 ps relaxation time in the present case is characteristic of defect-mediated recombination of excited carriers. The instantaneous response is believed to result from field-induced polarization of the material and, therefore, reflects the pulse duration employed.

In conclusion, the nonlinear optical properties of Ge nanocrystals formed in silica by ion implantation and annealing were examined. The magnitude of the nonlinear refractive index $|n_2^{Ge}|$ was found to increase linearly with increasing ion fluence and to increase as the length of the excitation pulse increased. Values as high as $6.9\times10^{-13}\,\mathrm{cm^2\,W^{-1}}$ were measured for samples implanted with $3\times10^{17}\,\mathrm{Ge\,cm^{-2}}$ and measured with a 650 fs pulse. Relaxation of the nonlinearity was shown to exhibit two characteristic time constants, a fast component characteristic of the pulse duration, and a slower component with a relaxation time $\leqslant1$ ps. The latter is comparable to that reported for carrier recombination in ion-irradiated semiconductors, suggesting it may be a consequence of defect-mediated recombination of photoexcited carriers.

The authors would like to thank David Llewellyn for his help with TEM sample preparation and TEM analysis.

[1] S. Banerjee and D. Chakravorty, Appl. Phys. Lett. **72**, 1027 (1998).
[2] M. Y. Lee, T. S. Kim, and Y. S. Choi, J. Non-Cryst. Solids **211**, 143 (1997).
[3] D. Ricard, P. Roussignol, and C. Flytzanis, Opt. Lett. **10**, 511 (1985).
[4] J. M. Ballesteros, R. Serna, J. Solis, C. N. Afonso, A. K. Petford-Long, D. H. Osborne, and R. F. Haglund, Jr., Appl. Phys. Lett. **71**, 2445 (1997).
[5] W. Schrof, S. Rozouvan, E. Van Keuren, D. Horn, J. Schmitt, and G. Decher, Adv. Mater. **3**, 338 (1998).
[6] H. B. Liao, R. F. Xiao, J. S. Fu, H. Wang, K. S. Wong, and G. K. L. Wong, Opt. Lett. **23**, 388 (1998).
[7] T. Inokuma, Y. Wakayama, T. Muramoto, R. Aoki, Y. Kurata, and S. Hasegawa, J. Appl. Phys. **83**, 2228 (1998).
[8] S. Vijayalakshmi, M. A. George, and H. Grebel, Appl. Phys. Lett. **70**, 708 (1997).
[9] N. R. Kulish, V. P. Kunets, and M. P. Lisitsa, Superlattices Microstruct. **22**, 341 (1997).
[10] E. Vanagas, J. Moniatte, M. Mazilu, P. Riblet, B. Honerlage, S. Juodkazis, F. Paille, J. C. Plenet, J. G. Dumas, M. Petrauskas, and J. Vaitkus, J. Appl. Phys. **81**, 3586 (1997).
[11] M. Zacharias, R. Weigand, B. Dietrich, F. Stolze, J. Blasing, P. Veit, T. Drusedau, and J. Christen, J. Appl. Phys. **81**, 2384 (1997).
[12] R. G. Elliman, B. Luther-Davies, M. Samoc, and A. Dowd, Mater. Res. Soc. Symp. Proc. **438**, 423 (1997).
[13] L. P. Yue and Y. Z. He, J. Appl. Phys. **81**, 2910 (1997).
[14] Y. Maeda, Phys. Rev. B **51**, 1658 (1995).
[15] Y. Kanemitsu, S. Okamoto, M. Otobe, and S. Oda, Phys. Rev. B **55**, R7375 (1997).
[16] A. Nakajima, Y. Sugita, K. Kawamura, H. Tomita, and N. Yokoyama, J. Appl. Phys. **80**, 4006 (1996).
[17] A. Pifferi, P. Taroni, A. Torricelli, G. Valentini, P. Mutti, G. Ghislotti, and L. Zanghieri, Appl. Phys. Lett. **70**, 348 (1997).
[18] S. Guha, M. D. Pace, D. N. Dunn, and I. L. Singer, Appl. Phys. Lett. **70**, 1207 (1997).
[19] F. P. Strohkendl, L. R. Dalton, R. W. Hellwarth, H. W. Sarkas, and Z. H. Kafafi, J. Opt. Soc. Am. B **14**, 92 (1997).
[20] M. Samoc, A. Samoc, B. Luther-Davies, Z. Bao, L. P. Yu, B. Hsieh, and U. Scherf, J. Opt. Soc. Am. B **15**, 817 (1998).
[21] T. Takagahara and K. Takeda, Phys. Rev. B **46**, 15578 (1992).
[22] S. M. Sze, *Physics of Semiconductor Devices* (Wiley, New York, 1969).
[23] A. Chin, K. Y. Lee, B. C. Lin, and S. Horng, Appl. Phys. Lett. **69**, 653 (1996).